ANALYSIS OF RELATIVE AIR/FUEL RATIO ON THE PERFORMANCE OF NATURAL GAS IC ENGINES

Dalton Bertoldi, dalton@polo.ufsc.br
Programa de Pós-Graduação em Engenharia Mecânica
Universidade Federal de Santa Catarina
88.040-900 – Florianópolis – Brasil

César J. Deschamps, deschamps@polo.ufsc.br
Amir A. M. Oliveira Jr., amir@emc.ufsc.br
Programa de Pós-Graduação em Engenharia Mecânica
Universidade Federal de Santa Catarina
88.040-900 – Florianópolis – Brasil

Abstract. *Natural gas is presented as an alternative to brazilian fuels market due to its gaseous polutants emission reduction potential. However, the use of an alternative fuel in the automotive industry requires a correct design of internal combustion engines. The present paper considers the development of a two-dimensional model to simulate a spark-ignition engine fuelled by a mixture of air and methane. The main goal is the analysis of relative air/fuel ratio effect on the engine performance, based on results for indicated power, volumetric efficiency and fuel conversion efficiency.*

Keywords*: internal combustion engine, natural gas, relative air/fuel ratio.*

1. INTRODUCTION

Recently, several researches have been carried out to analyze the use of natural as an alternative fuel for internal combustion engines. For example, Kato *et al.* (1999) developed an IC engine fuelled by compressed natural gas in order to reduce pollutants emissions levels. Valves opening conditions, fuel injection and exhaustion systems as well as compression ratio (from 9.5:1 to 11:1) were modified. Despite of such changes, the authors verified a decrease on maximum power (88 kW to natural gas against 97 kW to gasoline) and a decrease in the engine reliability due to high natural gas working temperatures and absence of lubrication on the valve seat, originally provided by the gasoline itself. However, pollutants emissions levels of the engine remained below the standard regulations.

Caillol *et al.* (2002) investigated the effect of natural gas composition variation on the burned mass fraction, flame velocity and pollutants emissions of a spark-ignition engine. A mono-cylindrical engine was tested with different relative air/fuel ratio (between 0.6 and 1.2) and four different natural gas compositions (from pure methane to ethane, propane and nitrogen gas mixtures). The authors concluded that a mixture of ethane and propane has a positive influence on flame velocity under poor combustion circumstances.

Tinaut *et al.* (2006) performed a numerical study to predict the performance of an IC engine operating with poor gas and other low calorific gaseous fuels, commonly obtained from solid biomass. A numerical simulation was considered for a 1.6 liters engine, with 9.6:1 compression ratio, and operating at 4,000 rpm with different fuels (poor gas, isooctane and methane). Tinaut *et al.* (2006) observed that indicated power for poor gas operating condition was 66%, and for methane was 85%, of the indicated power for gasoline operating condition.

Thobois *et al.* (2003) analyzed a spark-ignition engine operating with three different natural gas compositions and with isooctane, through a numerical simulation of a simplified axisymmetric geometry. The authors used correlations for the natural gas laminar flame speed to obtain the performance of a 1,750 cm^3 engine working with two different compression rates. Among the results obtained were combustion rate, in-cylinder pressure, turbulent intensity and indicated mean effective pressure. The results showed a 20% reduction on specific fuel consumption and a 5% loss on effective mean pressure for methane operation in comparison with isooctane fuelled condition. The gain obtained on specific fuel consumption was attributed, by the authors, to the higher hydrogen/carbon ratio presented on methane gas (4.00) when compared to isooctane (2.25).

The main goal of the present work is to analyze the relative air/fuel ratio effect on natural gas internal combustion engines performance, via numerical simulations of a small size spark-ignited internal combustion engine fuelled by different mixtures of air and methane. Methane gas is the major component of natural gas and more than 90% in volume of natural gas in Brazil and other countries is methane (Weaver, 1989). Since the low heating value of methane is similar to other hydrocarbons, the assumption of modeling natural gas as methane is a good approximation from the energy release point of view. However, it must be emphasized that small additions of larger hydrocarbons have a strong effect on the ignition behavior of natural gas (Westbrook *et al.*, 2005). However, the present study is neither focused on ignition analysis nor on abnormal combustion, but on the analysis of the effect of flow pattern and heat transfer on the IC engine performance.

2. PROBLEM FORMULATION

2.1. Geometry

The model for the intake, cylinder and exhaust systems rely on an axisymmetric two-dimensional approximation for a small size spark-ignited internal combustion engine fuelled by natural gas. The main cylinder dimensions and other engine characteristics are as follows: i) bore - 79.5 mm; ii) stroke - 80.5 mm; iii) connecting rod length - 129.025 mm; iv) crank radius - 40.25 mm; v) valves diameter - 30 mm; vi) valves lift - 10 mm; vii) compression ratio - 10:1.

The model considers the intake and exhaust valves aligned with the axis of the cylinder. Both the cylinder and piston heads are plane and parallel to each other. As a consequence of adopting a two-dimensional geometry, the intake has to be positioned in the cylinder head, whereas the exhaust was placed in the piston head. The piston motion was described according with the crankshaft mechanism. On the other hand, the displacements for the intake and exhaust valves were prescribed through polynomial functions, corresponding to model of a fixed valve command. The spark plug is located at the center of the intake valve surface. Intake and exhaust system are assumed to be connected to constant pressure reservoirs (*plenum*). Figure 1 shows a schematic view of the computational domain.

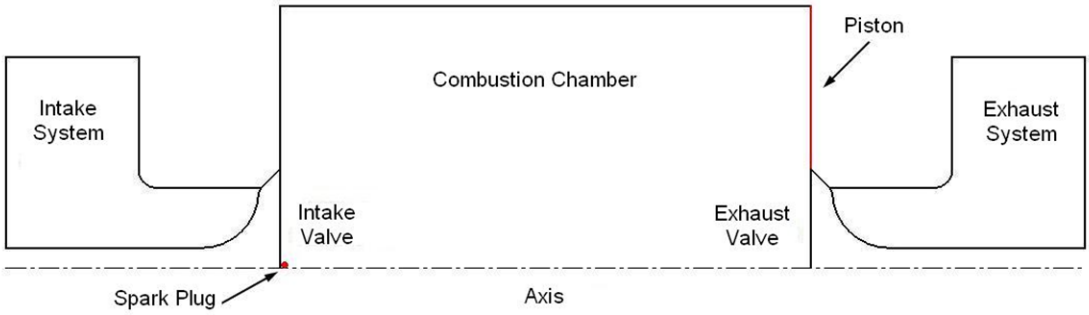

Figura 1. Rendering of the domain for the numerical simulations.

2.2. Governing equations

The chemical reaction is modeled as a global, one-step, chemical kinetic mechanism, with five chemical species. The mechanism for a stoichiometric combustion of methane with standard dry air, describes methane oxidation to create carbon dioxide and water vapor, as follows:

$$CH_4 + 2\left(O_2 + 3{,}76N_2\right) \rightarrow CO_2 + 2H_2O + 7{,}52N_2 \tag{1}$$

The fluid flow is modeled for an inertial frame of reference, with conservation equations for mass and momentum being coupled with conservation equations for thermal energy and mass of chemical species. Finally, a state equation for the ideal gas is also adopted to close the system of equations. Turbulence is modeled using the eddy viscosity concept through transport equations for the turbulent kinetic energy and its rate of viscous dissipation. The conservation equations are written in terms of Favre average (Peters, 2000). Thus, the equation for conservation of mass is

$$\frac{\partial}{\partial t}\overline{\rho} + \frac{\partial}{\partial x_i}\left(\overline{\rho}\widetilde{U}_i\right) = 0 \tag{2}$$

The conservation equation for the linear momentum, neglecting body forces, is written as:

$$\frac{\partial}{\partial t}\left(\overline{\rho}\widetilde{U}_i\right) + \frac{\partial}{\partial x_j}\left(\overline{\rho}\widetilde{U}_i\widetilde{U}_j\right) = -\frac{\partial \widetilde{P}}{\partial x_i} + \frac{\partial}{\partial x_j}\left(\mu_{eff}\frac{\partial \widetilde{U}_i}{\partial x_j}\right) \tag{3}$$

where $\overline{\rho}$ is the specific mass, $\widetilde{U}_i$ is the velocity vector, $\widetilde{P}$ is the pressure, $\mu_{eff}\left(=\mu+\mu_t\right)$ is the effective viscosity, written as the sum of molecular viscosity, μ , and turbulent viscosity, μ_t. The turbulent viscosity is evaluated through the RNG k-ε model (Orszag et al., 1993), which involves the solution of transport equations for turbulent kinetic energy $\widetilde{k}$ and for dissipation rate $\widetilde{\varepsilon}$ in order to estimate $\mu_t = C_\mu \rho k^2 / \varepsilon$.

The conservation equation for the mass of the chemical species *i* is written as:

$$\frac{\partial}{\partial t}\left(\overline{\rho}\widetilde{Y}_i\right)+\frac{\partial}{\partial x_j}\left(\overline{\rho}\widetilde{Y}_i\widetilde{U}_j\right)=\frac{\partial}{\partial x_j}\left[\left(\overline{\rho}D_{i,m}+\frac{\mu_t}{Sc_t}\right)\frac{\partial\widetilde{Y}_i}{\partial x_j}\right]+\widetilde{R}_i \tag{4}$$

where $\widetilde{Y}_i$ is the mass fraction of species *i*, $D_{i,m}$ is the molecular diffusion coefficient for species *i* in the mixture, Sc_t is the Schmidt turbulent number and $\widetilde{R}_i$ is the species production rate by chemical reaction.

The conservation equation for the thermal energy is expressed by Eq. (5):

$$\begin{aligned}\frac{\partial}{\partial t}\left(\overline{\rho}\sum_i\widetilde{Y}_i\widetilde{h}_i-\widetilde{P}+\frac{\overline{\rho}\widetilde{u}^2}{2}\right)+\frac{\partial}{\partial x_j}\left[\widetilde{U}_j\left(\overline{\rho}\sum_i\widetilde{Y}_i\widetilde{h}_i+\frac{\overline{\rho}\widetilde{u}^2}{2}\right)\right]=\\ \frac{\partial}{\partial x_j}\left[k_{eff}\frac{\partial\widetilde{T}}{\partial x_j}-\sum_i\widetilde{h}_i\left(\overline{\rho}D_{i,m}+\frac{\mu_t}{Sc_t}\right)\frac{\partial\widetilde{Y}_i}{\partial x_j}+\overline{\overline{\tau}}_{eff}\cdot\widetilde{U}_j\right]+\widetilde{S}_h\end{aligned} \tag{5}$$

where $\widetilde{h}_i$ is the enthalpy for each chemical species *j*, k_{eff} is the effective thermal conductivity of the fluid, $\overline{\overline{\tau}}_{eff}$ is the viscous stress tensor and $\widetilde{S}_h$ is the source term which includes heat generated by other volumetric heat source. The energy generated by combustion is already included in the mixture enthalpy, when a certain mass of reactants is transformed into products by chemical reaction.

The chemical reaction rate for species i is strongly non-linear and depends on local temperature and concentrations. To model the reaction rate, a chemistry-turbulence interaction mechanism is used and an average reaction rate is obtained. Here, the EDC (eddy-dissipation-concept) model (Magnussen and Hjertager, 1976; Magnussen, 1981, 1989) is adopted. In this model, it was assumed a complete molecular mixing of reactants and products within the smallest turbulent scales. In such small scales, called the inner region, there is a chemical reaction, controlled by a chemical reaction mechanism, transforming reactants into products as modeled by the global one-step mechanism presented in Eq. 1. Between the inner region and the outer region, there is a turbulent transport of reactants and products controlled by the turbulence large scales. The local mass balance requires that the net mass flux of each chemical species *i* between both regions (in and out) is equal to the inner region chemical reaction rate.

The volumetric fraction of the flow occupied by turbulent smaller scales (inner region) is given by ξ^3, where ξ is defined by:

$$\xi=C_\xi\left(\frac{\nu\varepsilon}{k^2}\right)^{1/4} \tag{6}$$

where C_ξ is a volumetric fraction constant equal to 2.1377 and ν is the kinematic viscosity.

Mass renewal inside the small scales region occurs in a time scale τ given by:

$$\tau=C_\tau\left(\nu/\varepsilon\right)^{1/2} \tag{7}$$

where C_τ is a time scale constant equal to 0.4082.

The net mass flux between the inner and outer of the region limited by the small scales results in the global reaction rate R_i:

$$R_i=\frac{\rho\xi^2}{\tau\left(1-\xi^3\right)}\left(Y_i^*-Y_i\right) \tag{8}$$

where Y_i^* is the mass fraction of chemical species *i* existing in the inner region. The model considered here assumes that the probability of reaction is equal to 1 (Magnussen, 1981; Magnussen, 1989).

The inner region mass balance requires that the net mass flux be proportional to the molecular chemical reaction rate, which means,

$$R_i^*=R_i/\xi^3 \tag{9}$$

The small scales region can be modeled as a perfect stirred reactor (PSR). Assuming a global, one-step, chemical kinetic mechanism as showed in Eq. (1), the mass and energy balances at small scales level result in

$$\frac{\rho^*}{\tau\left(1-\xi^3\right)}\left(Y_i^* - Y_i\right) = R_i^*, \qquad \frac{\rho^*}{\tau\left(1-\xi^3\right)}\left(h^* - h\right) = q^* \tag{10}$$

where ρ^* is the mixture specific mass of small scales region and h^* and h are the mixture enthalpies of small scales and mean flow regions given by:

$$h^* = \sum_1^N Y_i^* h_i^*, \qquad h = \sum_1^N Y_i h_i \tag{11}$$

where N is the number of chemical species present in the mixture (CH_4, O_2, N_2, H_2O e CO_2).

For the chemical reaction rate, we assume an Arrhenius model given by:

$$R_i^* = \frac{M_i}{n_i}\left[AT^{*\beta}\exp\left(-E/\overline{R}T^*\right)\right]X_{CH_4}^* X_{O_2}^{*\,2} \tag{12}$$

where A is the pre-exponential factor, E is the activation energy, β is a temperature coefficient, R is the universal constant of gas, M_i is the molecular mass of chemical species i and n_i is the stoichiometric coefficient of chemical species i in Eq. (1).

The gas mixture is assumed to follow an ideal gas behavior. Therefore,

$$p = \rho TR\sum_{i=1}^N \frac{Y_i}{M_i}, \qquad p^* = \rho^* T^* R\sum_{i=1}^N \frac{Y_i^*}{M_i} \tag{13}$$

$$h_i = h_{i,f}^o + \int_{T_o}^{T} c_{p,i}dT, \qquad h_i^* = h_{i,f}^o + \int_{T_o}^{T^*} c_{p,i}dT \tag{14}$$

where $c_{p,i}$ is the specific heat of chemical species i and $h_{i,f}^o$ is the standard enthalpy of formation.

The system of equations for the small scales is solved at each control volume, following a sub-grid model, providing results for temperature T^* and concentrations Y_i^*. Such results and the local mass fraction Y_i are then used to obtain the local average volumetric reaction rate from Eq. (8).

2.3. Boundary conditions

The solution domain adopts boundary conditions for pressure at the inlet of intake system and the outlet of exhaust system, corresponding to 101.3 kPa and 102.1 kPa, respectively. Turbulent intensity equal to 3% is assumed for an estimate of the turbulent kinetic energy k at both the inlet and outlet boundaries. The dissipation rate ε is evaluated from values for the turbulent kinetic energy and the length scale, which was assumed to be equal to the geometry hydraulic diameter.

At the inlet of the intake system, it was assumed the presence of a mixture of dry air and methane at 298 K. At the outlet of exhaust system, a locally parabolic flow condition with a completely burned mixture at 523 K was prescribed. The solid surfaces of the intake and exhaust system and the valve stem were considered to be adiabatic. On the other hand, the combustion chamber wall was considered to be isothermal, with a temperature value equal to 403 K. Ignition was applied through an energy deposition of 100, 200 or 300 mJ, depending on the mixture composition, and tested to take place at different crank angles. This deposition was applied during 10^{-4} s near the intake valve, in a circular region with a radius of approximately 2.0 mm.

The engine speed was set to 4,500 rpm, with the intake valve opening and closing at 0 and 224°, respectively, whereas for the exhaust valve such crank positions were 496° and 720°. Each simulation started with the piston in the top dead center (at zero crank angle degree) and finished in the same position (at 720 crank angle degree). A total of approximately 6 complete cycles were simulated so as to achieve a fully periodic regime operation.

The chemical reaction presented in Eq. (1) describes the combustion of a stoichiometric mixture of air and methane and, thus, defines the stoichiometric air/fuel ratio. Air/fuel ratios (*A/F*) simulated in the present work are: i) Stoichiometric (λ equal to 1.0 or A/F equal to 17.16); ii) Poor I (λ equal to 1.1 or A/F equal to 20.76); iii) Poor II (λ equal to 1.2 or A/F equal to 24.71).

3. NUMERICAL SOLUTION

The numerical solution of the conservation equations was obtained with the commercial code Fluent v.6.2.16 (2006), which is based on a finite volume methodology. The computational domain is divided into finite volumes that are used to integrate the differential equations by applying the Gauss Theorem in a collocated mesh arrangement. The pressure-velocity coupling is solved with the PISO algorithm. Proprieties at the volumes faces were interpolated with a first-order upwind scheme in the case of the energy equation and with a second-order upwind scheme balances of mass, momentum and species. Yet, for turbulence quantities the power-law scheme was adopted instead. The solution procedure was considered to be converged when the overall absolute residual on the control volumes was less than 10^{-3} for all the properties, except for the energy equation, for which the criterion was 10^{-6}.

The pressure fields for combustion chamber and intake system were initialized, respectively, with values of 102.1 and 101.3 kPa respectively. The initial temperature at the intake system was set to 298 K, while in the combustion chamber and exhaust system the initial temperatures were set to 700 K and 523 K, respectively. The mass fractions at the intake system were initialized with same values as fresh air/methane mixtures, depending on air/fuel ratio adopted. For the combustion chamber and the exhaust system values corresponding to total burned mixture were prescribed.

A very important aspect in numerical simulations is the assessment of truncation errors present in the solution, which is possible through tests of grid refinement. In the present work, this objective was reached by the simulation of a specific case using three different grids refine. The model was solved according with the conditions presented in section 2, with an ignition advance angle of 48° and a relative air/fuel ratio equal to 1 (stoichiometric). The computational grids denoted by 1, 2 and 3 are indicated in Tab. 1. The number of volumes for each grid changes according with the crank angle of the engine because a dynamic mesh is adopted.

Table 1. Number of volumes for numerical grid.

Number of Volumes	Minimum (top dead center)	Maximum (bottom dead center)
Mesh 1	5,990	20,830
Mesh 2	6,940	30,730
Mesh 3	8,500	49,290

As can be seen in Tab. 1, each grid has a maximum and a minimum number of volumes during the simulation of a complete engine cycle. Most of the refinements in the grids were directed to valve passages and to the in-cylinder region. Therefore, intake and exhaust systems remained with virtually the same grid refinement.

The size of the volume next to the wall in the cylinder region was kept the same for all computational grids. From this initial volume, the remaining volumes were then generated based on a geometric ratio of 1.15, allowing an increase of the volume size as a function of the distance from the wall.

Results for the engine performance obtained with the three grid refinements are presented in Tab. 2. As can be seen, the results are quite similar, with a difference less than 15% for the volumetric efficiency. Other results (indicated work, torque and power, fuel conversion efficiency and specific fuel consumption) showed variations of about 9.5%.

Table 2. Engine performance results according different grid refine.

Grid Refine	Grid 1	Grid 2	Grid 3
Volumetric efficiency	0.74	0.74	0.73
Indicated work [J]	335.8	344.5	361.4
Indicated torque [N.m]	0.47	0.48	0.50
Indicated power [kW]	12.59	12.92	13.55
Fuel conversion efficiency	0.33	0.34	0.36
Specific fuel consumption [g/kWh]	219.1	211.8	200.6

The simulations were carried out on a Pentium® IV 3.6 GHz with 2 Gb RAM memory. The numerical simulation time step was equal to 10^{-5} seconds to grid 1, while the time step was equal to 5×10^{-6} seconds to grids 2 and 3. Thus, grid 1 used 2,667 time steps, while grids 2 and 3 used 5,334 to achieve one complete cycle simulation. Due to these differences, grid 1 simulation spent 23 hours-simulation time, whilst grids 2 and 3 spent 48 and 72 hours-simulation time, respectively.

4. RESULTS

The effect of different relative air/fuel ratios on a natural gas IC engine was evaluated through a series of numerical simulations. Accordingly, three different ignition timings (48°, 54° and 60°) and three different relative air/fuel ratios (1,0, 1,1 and 1,2) were simulated using the same conditions presented in section 2. Each relative air/fuel ratio was simulated with three different ignition timings. The results for the engine performance according with these nine different operating conditions are presented in Tab. 3.

Table 3. Engine performance results according different relative air/fuel ratio.

λ	Ignition advance [°]	Volumetric efficiency	Indicated power [kW]	Fuel conversion efficiency	Specific fuel consumption [g/kWh]
1.0	48	0.74	12.55	0.33	219.96
	54	0.74	13.00	0.34	211.63
	60	0.74	10.87	0.28	252.29
1.1	48	0.75	10.83	0.31	232.74
	54	0.75	11.62	0.33	217.26
	60	0.74	12.42	0.35	202.88
1.2	48	0.75	8.66	0.27	267.98
	54	0.75	9.50	0.29	245.00
	60	0.75	10.59	0.33	219.66

As shown in Tab. 3, the maximum brake torque (MBT) is only reached for λ = 1.0. Unfortunately, the number of simulated cases with λ = 1.1 and 1.2 was not enough to allow one to clearly identify the maximum brake torque. As the ignition advance is increased, the engine power rises and the specific fuel consumption decreases. Consequently, there is an improvement in the fuel conversion efficiency, with the exception for the case corresponding to λ = 1.0 and ignition advance of 60°. For poor mixtures, it is observed an increase in the fuel conversion efficiency as the relative air/fuel ratio becomes higher than 1.0.

The combustion of poor mixtures originates lower temperature products (Heywood, 1988). This aspect can also be seen in the present study, from results for temperature of burned gases at different relative air/fuel ratio and 48 CAD BTDC ignition timing, as shown in Fig. 2. Before the opening of the discharge valve, the temperature of burned gases is smaller in the case of poorest mixtures. However, after the valve opening, this situation is inverted.

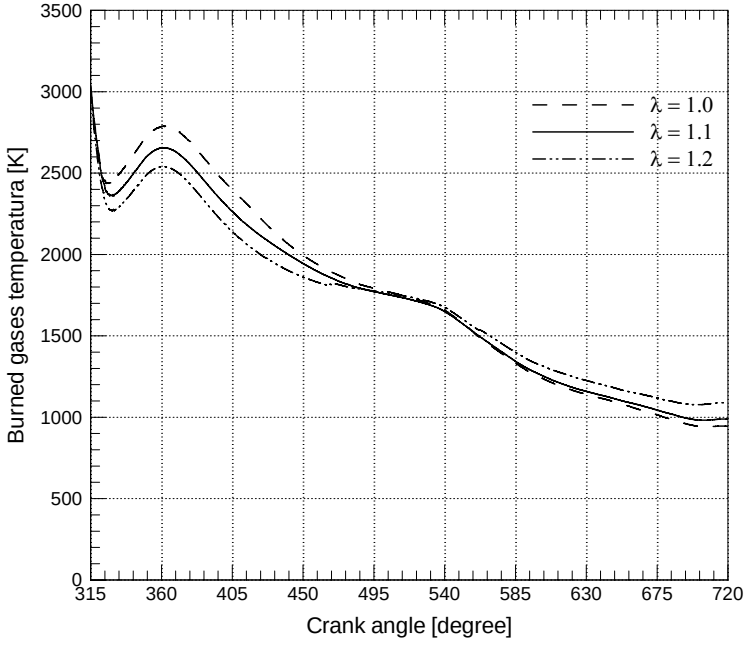

Figure 2. Burned gases temperature according crank angle.

The temperature increase verified for the burned gases of poorest mixtures during the valve opening is associated with the highest combustion rate. This is so because the combustion process in the poor mixtures considered here was not finished when the exhaust valve was closing. Therefore, the temperature of burned gases is higher than that

associated with λ = 1.0. This fact can be verified through oxygen destruction rate and carbon dioxide formation rate showed in Fig. 3. Considering carbon dioxide formation rate based on evaluation of reaction rate, the overall burning angle for λ = 1.0 is equal to 108°, while for λ = 1.1 and 1.2 such angles are 128° and 162°, respectively.

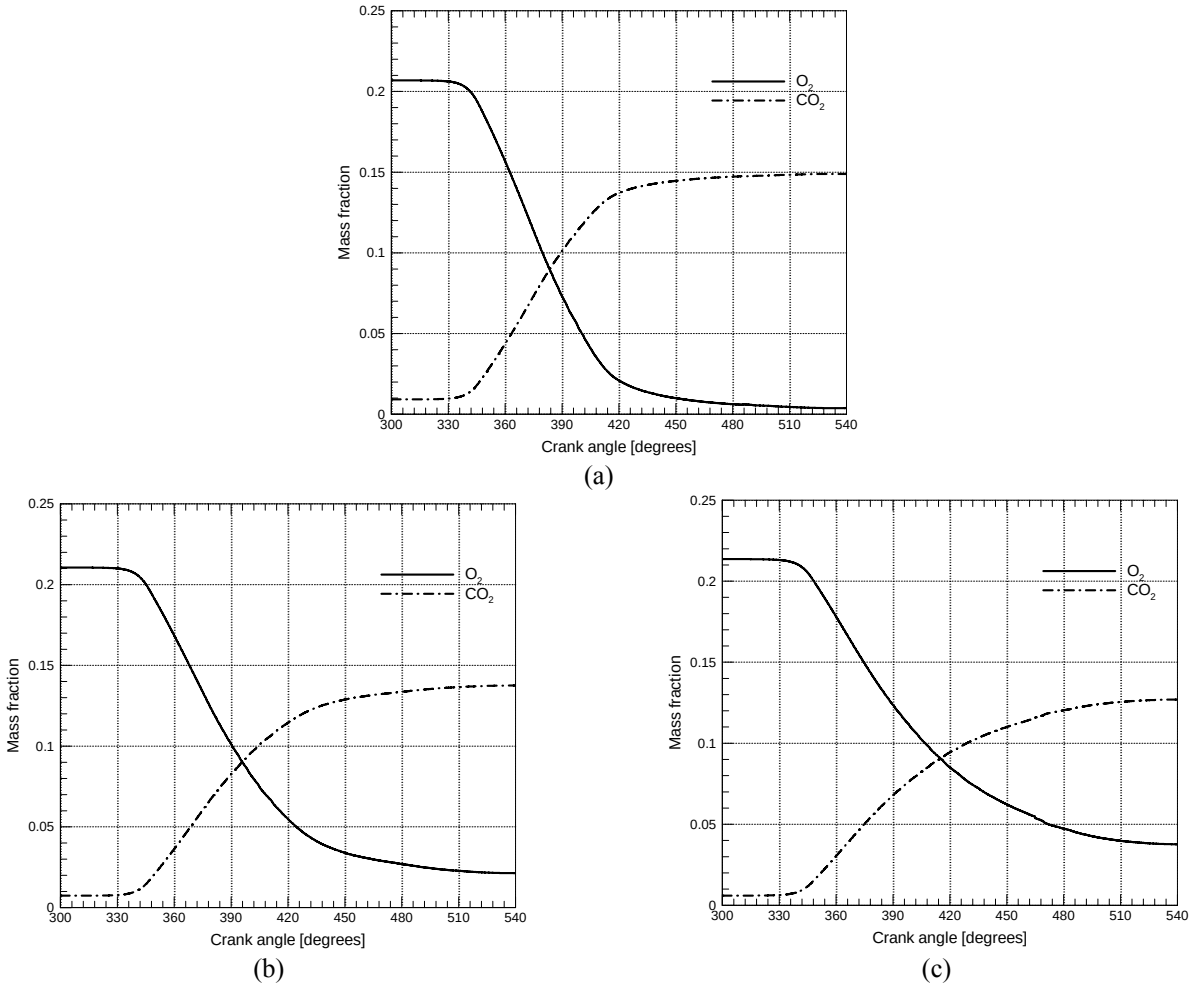

Figure 3. Mass fraction of O_2 and CO_2 according crank angle:
(a) λ equal to 1.0, (b) λ equal to 1.1 and (c) λ equal to 1.2.

5. CONCLUSION

The present work showed an analysis of the relative air/fuel ratio effect on natural gas IC engines performance through the numerical simulation of a simplified geometry, in order to reduce computational processing time. Grid refinement tests were also tested for an assessment of truncation errors in the numerical solution. Numerical results for the effect of relative air/fuel ratio were in agreement with data in the literature. As the relative air/fuel ratio is increased the mixture will be more diluted and, as a consequence, there will be a decrease in both the combustion rate the flame propagation speed. Therefore, the engine requires an increase in the ignition advance to achieve the same indicated power returned by a stoichiometric relative air/fuel ratio.

6. ACKNOWLEDGEMENTS

The authors acknowledge the support received from CAPES (Coordination for the Improvement of High Level Personnel).

7. REFERENCES

Akansu, S. O., Dulger, Z., Kahraman, N. and Veziroglu, N., 2004, "Internal combustion engines fueled by natural gas – hydrogen mixtures", International Journal of Hydrogen Energy, Vol. 29, pp. 1527-1539.

Caillol, C., Delorme, T., Denis, P. and Berardi, G., 2002, “A combustion model for analyzing the effects of natural gas composition on the operation of a spark ignition engine”, SAE paper 2002-01-2236.
Das, L. M., Gulati, R. and Gupta, P.K., 2000, “A comparative evaluation of the performance characteristics of a spark ignition engine using hydrogen and compressed natural gas as alternative fuels”, Internal Journal of Hydrogen Energy, Vol. 25, pp. 783-793.
Heywood, J. B., 1988, “Internal Combustion Engine Fundamentals”, New York: McGraw-Hill Inc.
Kato, K., Igarashi, K., Masuda, M., Otsubo, K., Yasuda, A., Takeda, K. and Sato, T., 1999, “Development of engine for natural gas vehicle”, SAE paper 1999-01-0574.
Magnussen, B. F. and Hjertager, B. J., 1976, On Mathematcal Modeling of Turbulent Combustion with Special Emphasis on Soot Formation and Combustion.16th Symp. (Int.) on Combustion (1976). Comb. Inst., Pittsburg, Pennsylvania, pp.719-729.
Magnussen, B. F., 1981, On the Structure of Turbulence and a Generalized Eddy Dissipation Concept for Chemical Reaction in Turbulent Flow. 19th AIAA Aerospace Science Meeting, Jan. 12-15, St.Louis, Missouri.
Magnussen, B. F., 1989, Modeling of NOx and soot formation by the Eddy Dissipation Concept. Int.Flame Research Foundation, 1st topic Oriented Technical Meeting. 17-19 Oct, Amsterdam, Holland.
Orszag, S. A., Yakhot, V., Flannery, W. S., Boysan, F., Chouhury, D., Maruzewski, J. and Patel, B., 1993, “Renormalization group modeling and turbulence simulations”, In: So, R.M.C., Speziale, C.G., & Launder, B.E., Near-Wall turbulent flows, Elsevier Science Publisher.
Peters, N., 2000, “Turbulent Combustion”, Cambridge University Press, Cambridge.
Thobois, L., Lauvergne, R., Gimbres, D. and Lendresse, Y., 2003, “The analysis of natural gas engine combustion specificities in comparison with isooctane through CFD computation”, SAE paper 2003-01-0009.
Tinaut, F. V., Melgar, A., Horrillo, A. and De La Rosa, A. D., 2006, “Method for predicting the performance of an internal combustion engine fuelled by producer gas and other low heating value gases”, Fuel Processing Technology, Vol. 87, pp. 135-142.
Weaver, C. S., 1989, “Natural gas vehicles – a part of the state of art”, SAE paper 892133.
Westbrook, C. K, Mizobuchi, Y., Poinsot, T. J., Smith, P. J. and Warnatz, J., 2005, “Computational combustion”, Proceedings of the Combustion Institute, vol. 30, pp. 125-157.

8. RESPONSIBILITY NOTICE

The authors are the only responsible for the printed material included in this paper.